Iraqi Journal of Physics, 2019 *Vol.17, No.42, PP. 65-75*
DOI: 10.20723/ijp.17.42.65-75

Investigation of the effect of post deposition thermal treatment on properties of P3HT and P3HT:PCBM blend

Abeer M. Musllim and Iqbal S. Naji

Department of Physics, College of Science, University of Baghdad

E-mail: moonbb_moonaaaa@yahoo.com

Abstract

This work reports the study of heat treatment effect on the structural, morphological, optical and electrical properties of poly [3-hexylthiophene] and its blend with [6,6]-phenyl C61 butyric acid methyl ester (P3HT:PC61BM). X-ray diffraction (XRD) measurements show that the crystallinity of the films increased with annealing. The evaluation of surface roughness and morphology was investigated using atomic force microscope (AFM), and field emission scanning microscope (FESEM). The optical properties were emphasized a strong optical absorption of P3HT compared with the blend. Hall effect measurement was used to study the electrical properties which revealed there is an increase in the electrical conductivity and Hall mobility of the p-type P3HT and its blend with heat treatment.

Key words
Organic semiconductor, fullerence blend, photovoltaic, polymer.

Article info.
Received: May. 2019
Accepted: Jun. 2019
Published: Sep. 2019

استقصاء تأثير المعاملة الحرارية بعد الترسيب على خصائص P3HT ومزيج P3HT:PCBM

عبير محمد مسلم و اقبال سهام ناجي

قسم الفيزياء، كلية العلوم، جامعة بغداد

الخلاصة

هذا العمل يوضح دراسة تأثير المعاملة الحرارية على الخصائص التركيبية ،السطحية، البصرية والكهربائية لمركب الهكساثيافين المتعدد (P3HT) ومزيجه مع حامض البيوترك مثيل استر(P3HT:PCBM). أوضحت قياسات حيود الأشعة السينية بان تبلور الأغشية ازداد مع التلدين. وتم استقصاء خشونة وتضاريس السطح باستخدام مجهر القوى الذرية (AFM) والمجهر الماسح ذي المجال الباعث (FESEM). الخصائص البصرية أوضحت امتصاص بصري قوي لمركب P3HT مقارنة مع المزيج. قياسات تأثير هول تم استخدامه لدراسة الخصائص الكهربائية والتي أوضحت بان التوصيلية الكهربائية وتحركيه هول للمركب P3HT نوع p وكذلك خليطه تزداد مع المعاملة الحرارية.

Introduction

The organic photovoltaics are promising alternatives to their inorganic counterparts [1]. They offer many practical advantages which that they can be simply prepared by solution processing techniques which in turn offer low fabrication cost and the potential to deposit on flexible substrates and they also have high absorption coefficients that offer possibility for production of very thin solar cells [2, 3]. But beside the advantages, it has disadvantages. The main one's is the low efficiency, low stability and low strength [3]. The most efficient conjugated polymer heterojunction devices use regioregular poly (3-hexylthiophene) (P3HT) as the electron donor due to its higher hole mobility 10^{-4} to 10^{-2} cm^2 V^{-1} s^{-1} and lower band gap [4, 5]. Also it is an important class of π-conjugation polymers which can be ordered in

three dimensions: the conformational ordering along the backbone, π-stacking of flat polymer chains and lamellar stacking between chains. All these features lead to the excellent electrical properties of this material [6]. Usually the polymer, electron donor, is blended with the electron acceptor, (6, 6)-phenyl-C61-butyric acid methyl ester (PCBM) [7], due to its high electron affinity, high solubility in organic solvents, and better electron mobility as compared to C60 [8, 9]. In P3HT:PCBM heterojunction devices, the ultrafast photoinduced charge transfer of the electron through PCBM and hole transfer via the backbone of P3HT polymer networks produce considerable solar energy conversion efficiency. In fact, efficiencies approach 5–6% [10, 11].

Thermal annealing have proved critical for optimizing the nanomorphology of a BHJ. Even though, significant improvements in PCE has been observed in the optimally annealed devices, precise control has to be imposed due to the sensitivity of the device performance towards annealing conditions [12]. The Selection of the solvent is also very important for obtaining good morphology of the films and stability of the photovoltaic device [13].

In this work, we have studied the effect of thermal annealing on the structural, morphological, and optical properties of P3HT and P3HT:PC61BM blend thin films.

Experimental procedure

Poly (3-hexylthiophene) (P3HT) with a molecular weight of 34.000 gm/mol and [6,6]-phenyl-C_{61}-butyric acid methyl ester (PCBM) were purchased from American Dye Source, Inc. and used without further purification. The solution of P3HT is made by dissolving 60mg of P3HT polymer powder in 2 ml of 1,2Dichlorobenzene ($C_6H_4CI_2$) with a molecular weight of 147.00 gm/mol which is a colorless to pale yellow liquid with a pleasant odor. The blend solution was also prepared by mixing 30mg of P3HT and 30mg of PCBM (1:1) weight ratio and dissolving in 2ml of 1,2Dichlorobenzene solvent. The two solutions were sonicated for 60 min in ultrasonic bath followed by hot plate stirring at 50^{o}C for 2 hours and 18 hours without heating to obtain homogenous solutions. Finally the both solutions were filtered by PTFE filter with a pore size of 0.45 μm to remove any un dissolve material and got homogenous solutions. Glass substrates were cleaned in an ultrasonic bath by using acetone and isopropanol then rinsed with deionized water and dried with nitrogen gas.

The P3HT and P3HT:PCBM blend thin films were spun on substrates by spin coating system (ACE200) with speed of 1000 rpm/S for 30 second. The thickness of pristine and blend films were measured by cross section method which was about (100, and 150 nm) respectively. The films were thermally annealed at different annealing temperatures (75, 100, 125, and 150^{o}C). All experimental processes were carried out in air without glove box. The microstructure of films were recorded at room temperature using X-ray diffraction system (SHIMADZU,XRD-6000) with CuKα radiation(λ=0.154 nm, current 30 mA, voltage 40 kV).The morphological features for P3HT and P3HT:PCBM blend were performed by using field emission scanning electron microscopy (FE-SEM) model (Hitachi 4700 field emission microscope),and atomic force microscopy(CSPM-AA3000 contact mode spectrometer, Angstrom Advanced Inc. Company). The optical properties were measured using UV-Visible SP-8001

spectrophotometer (Meterrech). The electrical properties was carried out using Hall Effect measurement system (HMS-3000, VER 3.5).

Results and discussion

The X-ray diffraction patterns of as deposited and annealed P3HT films are shown in Fig.1. A single diffraction peak with a reflection (100) was observed before annealing at 2θ=5.51° which is associated with the inter digitation of the alkyl chains of P3HT, while the heat treated samples at 100 and 150 °C shows a diffraction peak at 5.49° and 5.43° respectively, which is associated with the lamella structure of thiophene rings in P3HT. The same results of X-ray diffraction patterns are found by other researchers [14, 15].

The peak intensity increased with increasing the heat treatment temperature from room temperature to 150 °C, and there is a shift to lower 2θ angle and reduction in full width at half maximum was observed. This indicate there is an increase in the crystallites size. The d-spacing were estimated from Bragg's law and the crystallites size were calculated by the Scherrer equation and all are listed in the Table 1.

However, when P3HT blended with $PC_{61}BM$ as shown in Fig. 2. The X-ray diffraction spectra for as-deposited and annealed samples shows a low peak intensities at 5.41°, 5.44° and 5.45° which is associated with (100) reflection and corresponds to an ordered lamellar structure with an interlayer spacing which is formed by parallel stacks of P3HT main chains that are separated by regions that are filled with alkyl side chains [16].

The X-ray results indicate that the peak intensity of P3HT:$PC_{61}BM$ with a reflection of (100) plane was decreased slightly when the annealing temperature increase to 150 °C. There is a reduction in (FWHM) and an increase in crystallite size when the samples are heat treated at 100 and 150 °C.

It can be clearly seen from the all figures and table, the peak intensity of the blend (P3HT:$PC_{61}BM$) is reduced relative to the P3HT. This is probably due to the addition of fullerene molecules which perturbs the formation of P3HT crystallites, also due to amorphous nature of PCBM [17]. P3HT has the ability to crystallize and has a stabilizing effect on blend morphology [18, 19]. In the blend, crystalline P3HT gets interconnected with amorphous PCBM.

The crystallites size of all samples increased upon annealing at 100 and 150 °C. The minimum crystallite size was 8.98, and 13.04 nm for the as-prepared P3HT, and P3HT: $PC_{61}BM$ respectively. This result of decreasing in the crystallite size of P3HT films compared to the blend films agree with Van Heerden [20].

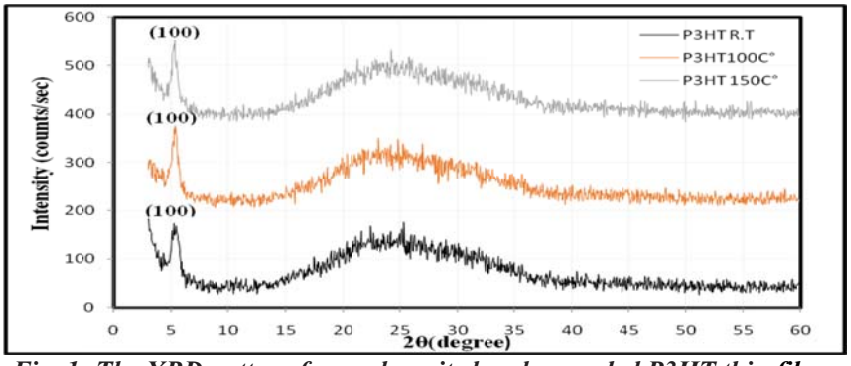

Fig. 1: The XRD pattern for as-deposited and annealed P3HT thin films.

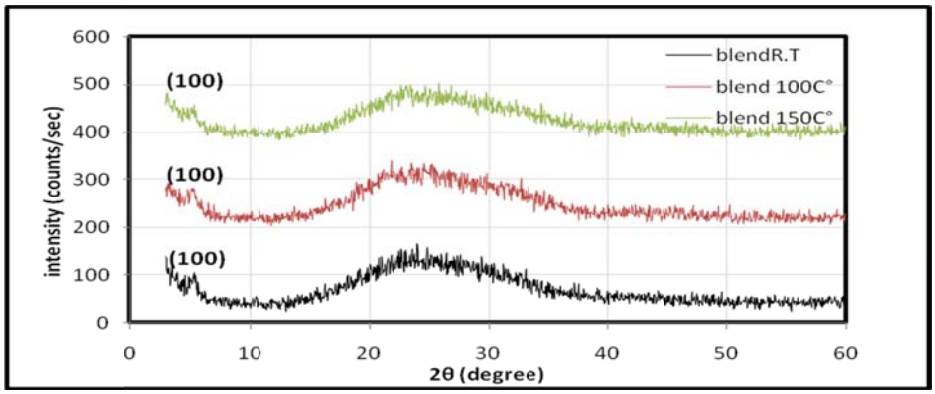

Fig. 2: The XRD pattern for as-deposited and annealed P3HT:PC61BM thin films.

Table 1: The structural parameters of P3HT and its blend thin films.

Sample	T_a(°C)	2θ(deg.)	d_{hkl} Exp. (nm)	d_{hkl} Theo. (nm)	hkl	FWHM (deg.)	C.S (nm)
P3HT	R.T	5.51	1.601	1.60	100	0.8857	8.98
	100	5.49	1.607	1.63	100	0.6013	13.22
	150	5.43	1.624	1.63	100	0.5596	14.21
P3HT:$PC_{61}BM$	R.T	5.41	1.629	1.63	100	0.6100	13.04
	100	5.44	1.622	1.63	100	0.5625	14.158
	150	5.45	1.617	1.63	100	0.5250	15.151

The variation in the surface morphology of P3HT and its blend films as a function of annealing temperature was evident as demonstrated in both AFM, as shown in Figs.3 and 4.

The as-deposited P3HT film has revealed a small size and a large number of grains with a roughness mean square (rms) of 0.63 nm. However, when the sample heat treated at 100 and 150 °C the roughness becomes 0.324 and 1.24 nm respectively. The surface becomes rougher as the annealing temperature increased to 150 °C. It is known that the higher roughness sample is better for photovoltaic application because when the surface is rough, the total surface area is much bigger than the sample with low roughness [21]. Also the grains diameter increases with increasing annealing temperature. All parameter are listed in Table 2.

On the other hand, the blend of P3HT with $PC_{61}BM$ as shown in Fig.3, the surface of as deposited films has a large number of grains with roughness mean square (rms) of 0.26 nm, and it is becomes 0.387 and 0.517 nm for sample annealed at 100 and 150 °C respectively. This increase is due to the addition of fullerene (C_{61}), Also the grains diameter increases with increasing annealing temperature, as shown in Table 2. It can be clearly seen that the P3HT has higher grain size than the blend which is probably due to high degree of crystallinity and self-organization beside that reason the annealing temperature increases the crystallinity of P3HT. And the rough surface of blend is probably a signature of polymer reorganization. However, the negative result of these morphological changes is that large grain features in P3HT:$PC_{61}BM$ can lead to a reduced charge collection rate at the electrodes. This is due to excessively long conduction path lengths compared to typical exciton diffusion lengths of 10 nm [22]. Since clustering of blends molecules with large grain features creates an inefficient conduction path for conjugated polymer chains to the

contact electrodes, charge carrier mobility's in conjugated polymers will be diminished and result in smaller photocurrent available necessary for efficient device operation. It should be noticed that Wobkenberg et al. [23], have already shown that C_{61} fullerenes combined with regioregular polymers can have comparable electron mobilities. So, small grain features with enhanced crystallinity in P3HT:PC_{61}BM nanocomposite films might offer better energy conversion efficiency of photoinduced carriers. This suggests that there is a thermodynamic driving force for the sample to reorganize towards a more stable equilibrium and thus to phase separate. However, excessive roughness makes phase segregation excessively comparable to the exciton diffusion length, which leads to the reduced charge segregation and device efficiencies. Similar results were also observed by Li et al. [24].

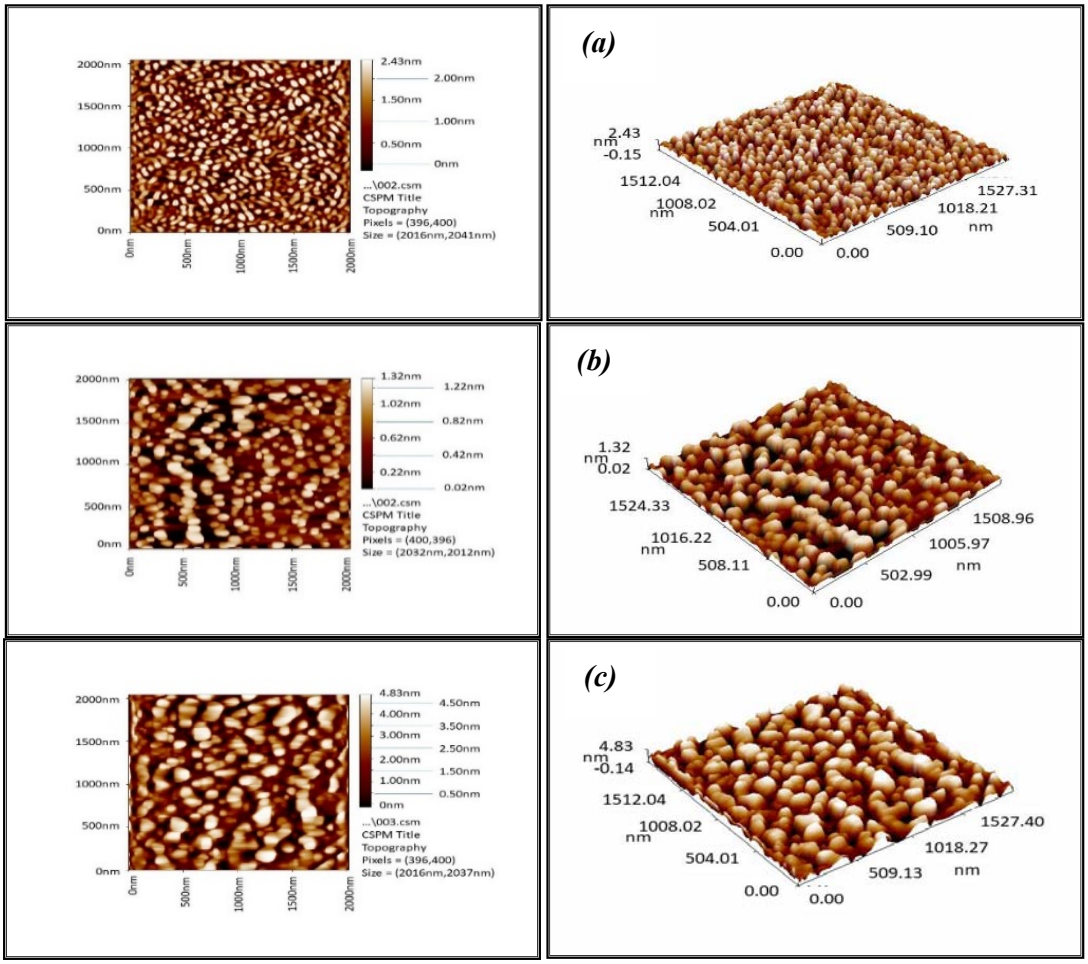

Fig. 3: AFM images of spin coated P3HT thin films at (a) as-deposited thin film (b) Ta=100 ˚C (c) Ta=150 ˚C.

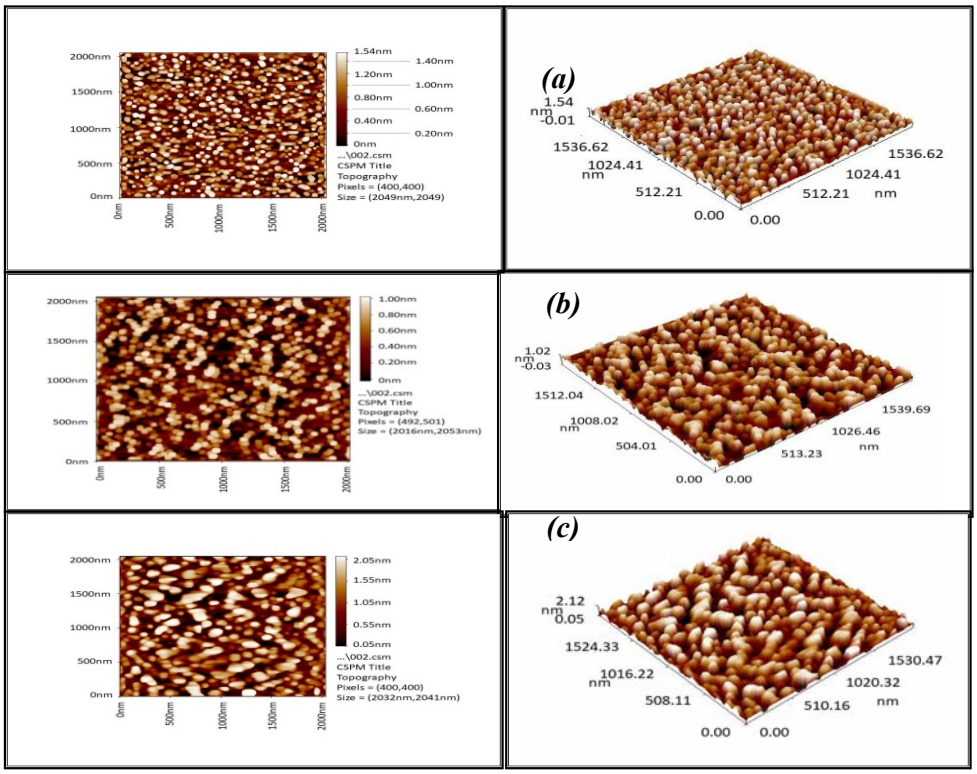

Fig. 4: AFM images of P3HT:PC$_{61}$BM thin films at (a) as-deposited thin film (b)Ta=100 ˚C (c) Ta=150 ˚C.

Table 2: Grain size, Roughness average, and root mean square of as deposited and annealed films.

Sample	T_a (°C)	Grain size (nm)	Roughness average (nm)	Root mean square (nm)
P3HT	R.T	68.62	0.63	0.731
	100	84.34	0.324	0.374
	150	114.25	1.24	1.43
P3HT:PC$_{61}$BM	R.T	70.04	0.26	0.299
	100	64.02	0.387	0.447
	150	97.86	0.517	0.597

Fig.5(a) display the scanning electron microscope images of pristine P3HT film deposited on glass substrate at room temperature by spin coating with different magnification. These images show a smooth and homogenous morphology with small cubic crystals. While Fig.5(b) shows the morphology of P3HT:PC$_{61}$BM blend film. It can be notice the surface has revealed some spherical- like features besides the cubic crystals which were attributed to the formation of PCBM aggregates. Such aggregation could form due to phase separation. These spherical-like nano scale PCBM aggregations could reduce the interface between P3HT and PCBM and therefore reduce the connected domains. In this case most of the generated charges will recombine before reaching the electrodes and will not contribute to the photocurrent.

Similar aggregations of PCBM in P3HT: PCBM film were observed by other researchers [25].

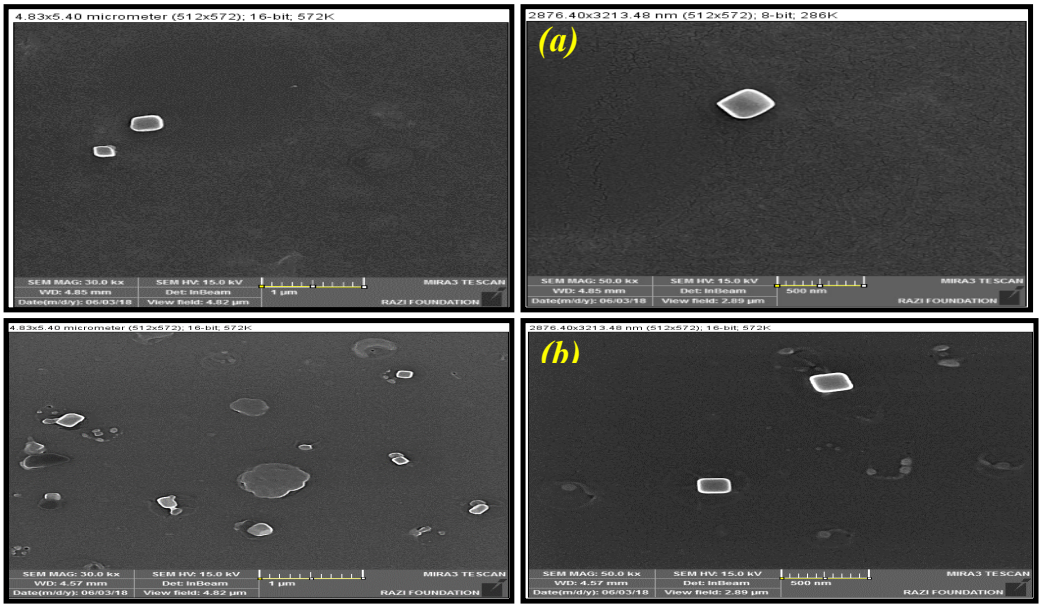

Fig. 5: FESEM pictures of (a) P3HT, (b)P3HT:$PC_{61}BM$ film at room temperature.

Fig.6(a) shows the UV-vis absorption spectra of P3HT thin films at different annealing temperature. It can be observed that the P3HT film exhibits strong absorption in the visible wavelength range from 400-650 nm. Generally, pristine P3HT and annealed films at different annealing temperature shows a maximum absorption around the wavelength of 555nm and a shoulder peak around the wavelength of 515 nm. These bands absorption can be attributed to the π-π* electronic transition of the P3HT conjugated backbone system [26]. While the shoulder peak around 610 nm could be related to the interchain stacking of P3HT molecules which suggested an enhancement in the chain ordering of the polymer [27]. It can also observed that there is no shift in the absorption peaks when the films are heat treated at different annealing temperature. But only a significant increase in the absorption intensity with increasing the annealing temperature and reach a maximum value for sample annealed at 100 °C which increase from 61 % at room temperature to 69 %. Which is indicated an increase in crystalline ordering of the polymer domain [28].

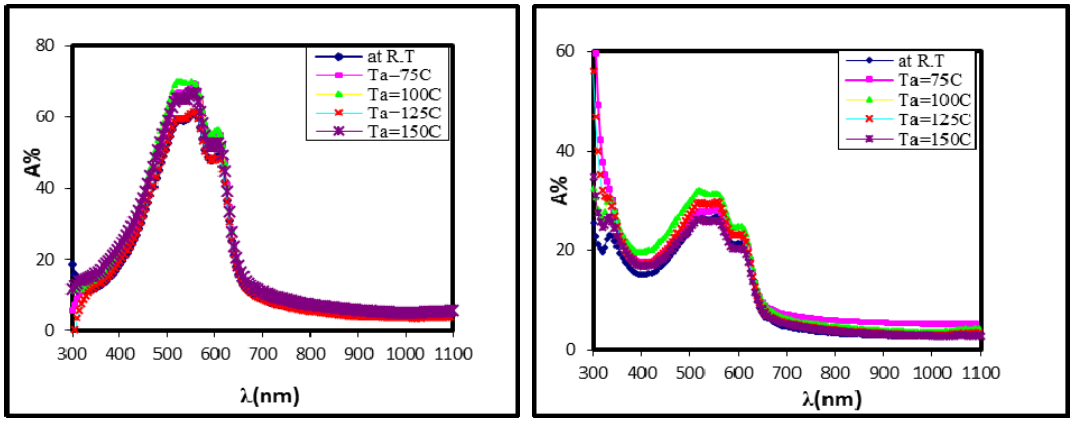

Fig. 6: The absorbance spectra of (a) P3HT and (b) P3HT:$PC_{61}BM$ thin films at different annealing temperatures.

When P3HT is blended With $PC_{61}BM$, as shown in Fig.6(b) the absorption spectra of the blend has a broad peak which originates from P3HT and ranges from 450 to 650 nm. The sharp peak which is generated from $PC_{61}BM$ and located at 330 nm represent prominent peak in the polymer (P3HT) which improve the π-π stacking of the polymer chains. The spectral region associated with P3HT absorption shows three absorption bands, the maximum absorption peak around the wavelength of 550 nm which is attributed to the π-π* electronic transition within the P3HT main polymer [25]. And two shoulders peaks at 515 nm and the second at 610 nm is attributed to the absorption of the interchain stacking of P3HT and which suggest an improvement in the ordering of the chain [29]. It can be clearly seen that the P3HT peaks remain unchanged before and after heat treatment, whereas in the region of PCBM absorption a slight red shift from 295 nm to 330 nm becomes evident.

However, all figures show a reduction in absorption intensity of the blend compared with the P3HT before and after annealing .This reduction in intensities might be due to a tighter chain which produced by twisting of the polymer backbone or due to broken conjugation in the presence of C_{61}, thereby causing in a segments with a shorter conjugation length and weaker interchain interaction. This result can also be explained by a change in the stacking conformation of the P3HT structure from high crystallinity to lower crystallinity , and a reduction of intraplane and interplane stacking, which causes a poor π-π* transition and lower absorbance. This reduction in intensities was also observed in the literature [30].

Fig.7(a) shows the optical energy gap of as deposited and annealed P3HT at different annealing temperature. It can be observed that there is a reduce in optical energy gap of P3HTwhen the sample are heat treated. This results of decreasing in optical energy gap in P3HT films when applying heat to the samples has also observed by other researchers Xiaoyin et al. [31]. Thus, the annealing process could be a method in reducing the optical energy gap of P3HT.

Fig.7(b) shows the variation of energy gap when P3HT is blended with $PC_{61}BM$ at different annealing temperature. It can be observed that the optical energy gap decreases after heat treatment to minimum value (1.84 eV) at 100 $^{\circ}$C, and return to its origin value (1.9 eV) when the annealing temperature equal to 150 $^{\circ}$C. While the energy gap of PCBM was 3.2 eV.

The reduction in energy gap is one of the crucial factors to obtain a good performance in the polymeric solar cells, in which that many photons can be absorbed in the active layer to generate charge carriers [32, 33].

Table 3 shows all the optical parameters of P3HT and its blend thin films at different annealing temperatures.

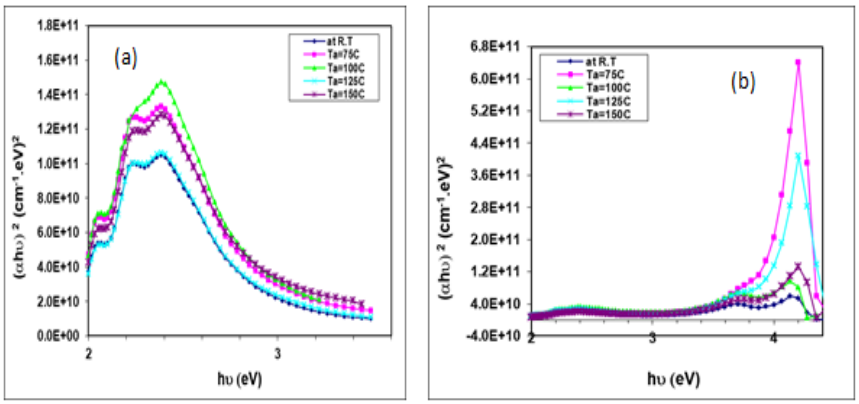

Fig.7: $(\alpha hv)^2$ versus photon energy (hv) of incident radiation for (a) P3HT and (b) P3HT:$PC_{61}BM$ thin films at different annealing temperatures.

Table 3: The optical constants of P3HT and P3HT:$PC_{61}BM$ thin films with different annealing temperatures at λ=550 nm.

Sample	Temp. (°C)	E_g^{opt}(eV)	α(cm^{-1}) *10^4	n	k	ε_r	ε_i
P3HT	25	1.90	14.0	1.990	0.612	3.585	2.438
	75	1.88	15.8	1.501	0.690	1.778	2.075
	100	1.86	16.1	1.278	0.704	1.137	1.801
	125	1.87	15.3	1.673	0.670	2.350	2.242
	150	1.89	15.3	1.978	0.615	3.535	2.433
P3HT:$PC_{61}BM$	25	1.90	6.13	2.526	0.268	6.311	1.356
	75	1.88	6.50	2.548	0.284	6.415	1.449
	100	1.84	7.25	2.578	0.317	6.545	1.635
	125	1.85	6.81	2.563	0.298	6.483	1.529
	150	1.90	5.98	2.515	0.261	6.261	1.317

In order to determine the electrical conductivity, resistivity, type and concentration of the carrier, and hall mobility, Hall Effect is used.

Table 4 illustrates the main parameters estimated from hall effect measurements for P3HT thin films deposited at different annealing temperature 100 and 150 °C. the result showed that all films were P type. It can observe that the conductivity and hall mobility are increase as the annealing temperature increases. since the mobility is a function of degree of crystallinity, crystallite size and phase domain size which are called the morphological variables, it can be concluded that the enhancement of mobility is attributed to the improvement in the crystallinity and morphology as observed in XRD, SEM and AFM analysis [34]. while the carriers concentration are decrease with heat treatment of the sample.

For P3HT blending with $PC_{61}BM$, it can be observed that there is an increase in the conductivity and the hall mobility of the blend with the increase of annealing temperature. Such an increase, may be attributed to enhanced polymer ordering. while the carriers concentration decrease. The blend films has higher conductivity and carrier mobility compared with the P3HT films.

It is assumed that the improved electrical properties of the blends are induced by smaller polymer and

fulleren clusters formed during spin coating, which lead to the development of continuous pathways for charge carriers and an increase in the interfacial area that inhanced the exciton dissociation [16].

Motaung et al. [16] reported that there is an increase in the Hall mobility and coductivity of P3HT and blened films after short time annealing. especially in the case of the blends. since fullerene crystallizes out of the polymer matrix under optimized annealing conditions ,leaving the polymer chains behind that will endeavour to recoganize and obtain an obtimized morphology.

Table 4: The electrical measurements of pristine P3HT and P3HT:$PC_{61}BM$ thin films at different annealing temperatures.

sample	Ta (°C)	type	σ x 10^{-5} $(\Omega.cm)^{-1}$	n *10^{11} (cm^{-1})	μ *10^{2} $(cm^2/V.s)$
P3HT	R.T	P	0.3409	3.485	0.6105
	100 °C	P	0.4242	3.257	0.8130
	150 °C	p	0.6929	0.4555	9.495
P3HT:PC_{61}BM	R.T	P	0.3799	46.73	0.05075
	100 °C	n	0.3883	3.403	0.7123
	150 °C	P	0.4693	39.31	0.07452

Conclusions

The post deposition heat treatment has induced significant changes in the properties of the thin films, where the ability to control the heat treatment to obtain enhanced crystallinity and optimal morphology properties and increases the electrical conductivity to improve the efficiency of the organic solar cell. The heat treatment improves the crystallinity, and the natural tendency of regioregular P3HT to crystallize is disturbed by addition of PCBM. AFM analysis revealed a crystallite-like surface morphology with crystallite size in the nanometer rang. The UV-Vis results show that the best annealing temperature for higher absorbance was 100^{o}C for both P3HT and its blend. Hall Effect indicates an increase in the conductivity and mobility with increasing the annealing temperature. These changes were explained in terms of the formation of polymer crystallites upon annealing.

References

[1] S. Miller, Giovanni Fanchini, Yun-Yue Lin, Cheng Li, Chun-Wei Chen, Wei-Fang Su, Manish Chhowalla, Journal of Materials Chemistry, 18, 3 (2008) 306-312.

[2] Shen, Yang, Kejia Li, Nabanita Majumdar, Joe C. Campbell, Mool C. Gupta., Solar Energy Materials and Solar Cells, 95, 8 (2011) 2314-2317.

[3] Movla, Hossein, Amin Mohammadalizad Rafi, Nima Mohammadalizad Rafi., Optik, 126, 15-16 (2015) 1429-1432.

[4] Ludwigs, Sabine, ed. "P3HT Revisited-from Molecular Scale to Solar Cell Devices", Vol. 265, Berlin: Springer, 2014.

[5] Chen, Shilin, Wenjin Zeng, Xiaodan Su, Jin Wang, Danbei Wang, Hongmei Zhang., Materials Science in Semiconductor Processing, 39 (2015) 441-446.

[6] Jang, Yoonhee, Ji-Won Seo, Jeesoo Seok, Jung-Yong Lee, Kyungkon Kim., Polymers 7, 8 (2015) 1497-1509.

[7] I.Malti, A.Chiali, N.C. Sari, Applied Solar Energy, 52, 2 (2016) 122-127.

[8] Li, Cheng, Yuhong Chen, Yubing Wang, Zafar Iqbal, Manish Chhowalla, and Somenath Mitra., Journal of

Materials Chemistry, 17, 23 (2007) 2406-2411.
[9] He. Youjun and Yongfang Li., Physical Chemistry Chemical Physics, 13, 6 (2011) 1970-1983.
[10] Reyes-Reyes, Marisol, Kyungkon Kim, David L. Carroll., Applied Physics Letters, 87, 8 (2005) 083506.
[11] Park, Sung Heum, Anshuman Roy, Serge Beaupré, Shinuk Cho, Nelson Coates, Ji Sun Moon, Daniel Moses, Mario Leclerc, Kwanghee Lee, Alan J. Heeger., Nature Photonics, 3, 5 (2009) 297-302.
[12] Ramani, Ramasubbu, and Sarfaraz Alam., Polymer, 54, 25 (2013) 6785-6792.
[13] Rait, Sukhbinder, Shipra Kashyap, P. K. Bhatnagar, P. C. Mathur, S. K. Sengupta, J. Kumar., Solar Energy Materials and Solar Cells, 91, 9 (2007) 757-763.
[14] Jung, Jae Woong and Won Ho Ja. In World Renewable Energy Congress-Sweden, 8-13 May, 057 (2011) 2838-2845.
[15] D.E. Motaung, G. F. Malgas, Ch. J. Arendse, S.E. Mavundla, C. J. Oliphant, D.Knoesen, Journal of Materials Science, 44, 12 (2009) 3192-3197.
[16] D. E.Motaung, G.F. Malgas, C. J. Arendse. Journal of Materials Science, 46, 14 (2011) 4942-4952.
[17] S. Sahare, N. Veldurthi, S. Datar, T. Bhave., RSC Advances, 5, 124 (2015) 102795-102802.
[18] U. Zhokhavets, T. Erb, G. Gobsch, M. Al-Ibrahim, O. Ambacher, Chemical Physics Letters, 418, 4-6 (2006) 347-350.
[19] Y-H.Chen, P-T. Huang, K-C. Lin, Y-J.Huang, C-T. Chen., Organic Electronics, 13, 2 (2012) 283-289.
[20] B.A. Van Heerden, "Charge Transfer Efficiency and Optical Properties of P3ht/Pcbm Spin Coated Thin Films" Department Of Physics University of The Western Cape, 2009.
[21] N. S. M.Shariff and P. S. M. Saad, Student Conference on Research and Development (SCOReD), 2016 (2016) 1-4.
[22] Y.Yao, C. Shi, G. Li, V.Shrotriya, Q. Pei, Y.Yang. Applied Physics Letters, 89, 15 (2006) 153507-1_153507-3.
[23] P. H.Wöbkenberg, D. D. C Bradley, D. Kronholm, J. C. Hummelen, D. M. de Leeuw, M.Cölle, T. D. Anthopoulos. Synthetic Metals, 158, 11 (2008) 468-472.
[24] Gang Li, Vishal Shrotriya, Yan Yao, Yang Yanga, Journal of Applied Physics, 98 (2005) 043704-1_ 043704-5.
[25] B.Kadem, A. Hassan, W. Cranton, Journal of Materials Science, Materials in Electronics, 27, 7 (2016) 7038-7048.
[26] V. Shrotriya, J. Ouyang, R. J. Tseng, G. Li, Y. Yang. Chemical Physics Letters, 411, 1-3 (2005) 138-143.
[27] Kadem, Burak and Aseel Hassan. Energy Procedia, 74, (2015) 439-445.
[28] T. Erb, U.Zhokhavets, H.Hoppe, G. Gobsch, M.Al-Ibrahim, O. Ambacher, Thin Solid Films, 511 (2006) 483-485.
[29] Y. Sun, J-G Liu, Y. Ding, Y-C Han, Chinese Journal of Polymer Science, 31, 7 (2013) 1029-1037.
[30] D. E. Motaung, G. F. Malgas, C.J. Arendse. Synthetic Metals, 160, 9-10 (2010) 876-882.
[31] X. Xiaoyin, J. Heongkyu, Eun- L. Cheol, Journal of the Korean Physical Society, 57 (2010) 144-148.
[32] Klaus Petritsch, "Organic solar cell architectures" PhD Thesis. Cambridge and Graz (2000).
[33] S. Sun, Z. Fan, Y. Wang, J. Haliburton, Journal of Materials Science, 40, 6 (2005)1429-1443.
[34] D.E. Motaung, G. F. Malgas, C. J. Arendse, T. Malwela. Materials Chemistry and Physics, 124, 1 (2010) 208-216.